Geophysical Research Letters

RESEARCH LETTER
10.1029/2021GL093516

Key Points:

- Meander bend migration is described through a catch-up behavior, driven by intermittent bank collapse events
- As the river bend evolves increasing its apex curvature, bank collapse tends to occur at the location of maximum shear stress
- Individual bank collapse events speed up the short-term migration rate of meandering rivers

Supporting Information:

Supporting Information may be found in the online version of this article.

Correspondence to:
Z. Gong,
gongzheng@hhu.edu.cn

Citation:
Zhao, K., Lanzoni, S., Gong, Z., & Coco, G. (2021). A numerical model of bank collapse and river meandering. *Geophysical Research Letters*, *48*, e2021GL093516. https://doi.org/10.1029/2021GL093516

Received 23 MAR 2021
Accepted 24 MAY 2021

A Numerical Model of Bank Collapse and River Meandering

Kun Zhao[1,2], Stefano Lanzoni[3], Zheng Gong[1], and Giovanni Coco[2]

[1]State Key Laboratory of Hydrology-Water Resources and Hydraulic Engineering, Hohai University, Nanjing, China, [2]School of Environment, University of Auckland, Auckland, New Zealand, [3]Department of Civil, Environmental and Architectural Engineering, University of Padua, Padua, Italy

Abstract Meander migration results from the interaction between inner bank accretion and outer bank erosion/collapse. This interaction has been usually treated as a long-term average of a sequence of erosion events determined by flow hydrographs. Little attention has been paid to the role that individual bank collapse events play on meander evolution. To fill this gap, we developed a numerical model of river meandering that describes explicitly bank collapse. Results show that as bend curvature increases due to meander migration and elongation, the initially scattered locations of bank collapse events converge toward the channel section where bed shear stress attains a maximum. Simulations illustrate the observed catch-up behavior between inner and outer banks, driven by intermittent bank collapse events. Moreover, bank collapse is found to speed up short-term meander migration and, consistent with field observations, meanders turn out to evolve toward a state characterized by constant channel width.

Plain Language Summary Meanders are one of the most ubiquitous morphological features observed in natural rivers. They consist of a series of alternating bends that, seen from above, display one of the most striking morphological patterns in nature. The migration of meandering rivers is attributed to outer bank retreat, due to erosion, and inner bank accretion, due to deposition. In this work, we propose a morphodynamic model to investigate the effects that repeated bank collapse events have on meander evolution. Our results show that the migration of meander bends can be described through a catch-up behavior, driven by outer bank collapse and subsequent inner bank accretion, that on average ensures a nearly constant channel width.

1. Introduction

River meanders are one of the most distinctive features of fluvial environments, and for many years, the beauty of these ubiquitous loops have attracted the interest of scientists (see e.g., among many others, Howard, 1996; Parker et al., 2011; Seminara, 2006; Zolezzi et al., 2012). From an ecological and socio-economic perspective, the migration of meanders is commonly accompanied by drastic changes in the landscape, and therefore can be responsible for farmland and wetland loss (Darby & Thorne, 1994; Odgaard, 1987), damage of riparian infrastructures and hydraulic structures (Hackney et al., 2020; Hooke, 1979), and even modulation of diversity in species and vegetation units (Piégay et al., 2005).

The migration of meandering rivers is attributed to the mutual interaction between the intermittent erosion/collapse of the outer bank (the outer side of a river bend) and the continuous accretion of the inner bank (the inner side of a river bend) (Mason & Mohrig, 2019; Nanson & Hickin, 1983). Field evidence suggests that, when plotted against the radius of curvature, local migration rates grow gently as the radius decreases until reaching a maximum at a critical value of the bend curvature and then decreasing rapidly (Finotello et al., 2018; Furbish, 1988; Hudson & Kesel, 2000; Lagasse, Zevenbergen, et al., 2004; Nanson & Hickin, 1983). Past theoretical work on river meandering has been devoted to the development of a mathematical framework (bend theory) for meander morphodynamics (Blondeaux & Seminara, 1985; Frascati & Lanzoni, 2009; Ikeda et al., 1981; Lanzoni & Seminara, 2006; Zolezzi & Seminara, 2001). The bend theory describes the development of meanders as the result of a bend instability, given a migration rate usually related to the excess flow velocity driven by bend curvature (e.g., Ikeda et al., 1981). Two further assumptions characterize this theory, which describe in an averaged sense the actual processes: (a) a constant channel width, which implies that outer and inner bank processes are synchronous, and (b) a continuous and velocity-based bank erosion, implying that individual bank collapse events are neglected. Both assumptions arise from observations showing that meandering rivers, when averaged over the time-scale typical of meander migration, tend to maintain a constant width (Lagasse, Spitz, et al., 2004; Lopez Dubon & Lanzoni, 2019).

Recently, studies have been conducted to address the dynamics of each bank independently, and have focused on the relative importance of outer bank erosion versus inner bank accretion (Asahi et al., 2013; Darby et al., 2002; Eke, Czapiga, et al., 2014; Langendoen et al., 2016; Parker et al., 2011; Zolezzi et al., 2012). Although neglecting bank collapse, Eke, Parker, and Shimizu (2014) suggested the existence of various regimes of bank interaction: both banks eroding, both banks depositing, bar push (faster migration of the inner bank) and bank pull (faster migration of the outer bank), depending on the initial meander configuration and the soil parameters controlling erosion and deposition rates. A river bend can then switch from one regime to another as it evolves toward an asymptotic state where, eventually, both erosion and deposition are roughly equal. More recently, high-resolution field observations have captured a catch-up behavior between inner and outer banks, whereby the river bends widen and narrow in discrete steps, maintaining a statistically steady-state or "equilibrium" channel half width, B_{eq} (Mason & Mohrig, 2019). This provides inspiration to address the paradox of constant channel width, despite the independent and different migration of inner and outer banks.

As for the assumption of a velocity-based bank erosion, simplified representations of bank retreat, carried out at the laboratory scale, have suggested the importance of intermittent bank collapse events. Consequently, the retreat rate is related not only to the near-bank flow velocity, but is also affected by the ratio between bank height and near-bank water depth (Patsinghasanee et al., 2018; Samadi et al., 2013; Zhao et al., 2020).

Here we set up a morphodynamic model involving bank collapse, to describe the catch-up behavior of meander migration associated with the interrelated dynamics of inner and outer banks. Bank collapse is modeled though either a stress-strain analysis, or employing an empirical function derived from laboratory experiments. In order to shed light on the importance of a realistic representation of bank collapse, we focus on meander evolution until incipient cutoff. The results lead us to a conceptual framework of a catch-up behavior that explains the migration of meanders in relation to bank collapse.

2. Method

The mathematical set-up governing the planform evolution of meandering channels has been thoroughly described (Frascati & Lanzoni, 2013; Seminara, 2006). Here we briefly introduce the ingredients needed to model bank retreat and accretion.

Bank accretion is assumed to be determined only by sediment deposition, whereas bank retreat is given by the sum of flow-induced sediment erosion and gravity-induced bank collapse. Along the banks, sediment erosion and deposition are assumed to act independently and an excess shear stress formula is applied to each process:

$$\varepsilon_E = R_E M_e \left(\frac{\tau_b - \tau_c}{\tau_c} \right) \tag{1}$$

$$\varepsilon_D = R_D M_d \left(\frac{\tau_d - \tau_b}{\tau_d} \right) \tag{2}$$

Here ε_E and ε_D are the rates of bank erosion and deposition (m/s), M_e and M_d are the erosion and deposition coefficients (m/s), both set to 1×10^{-6} m/s, τ_b is the near-bank shear stress (Pa), τ_c, τ_d are the critical shear stresses for erosion and deposition (Pa), which are set to 3 and 10, respectively. R_E and R_D are proportionality coefficients introduced to probabilistically constrain channel width variations. Indeed, field observations have suggested that rivers tend to maintain a nearly constant width as they migrate laterally

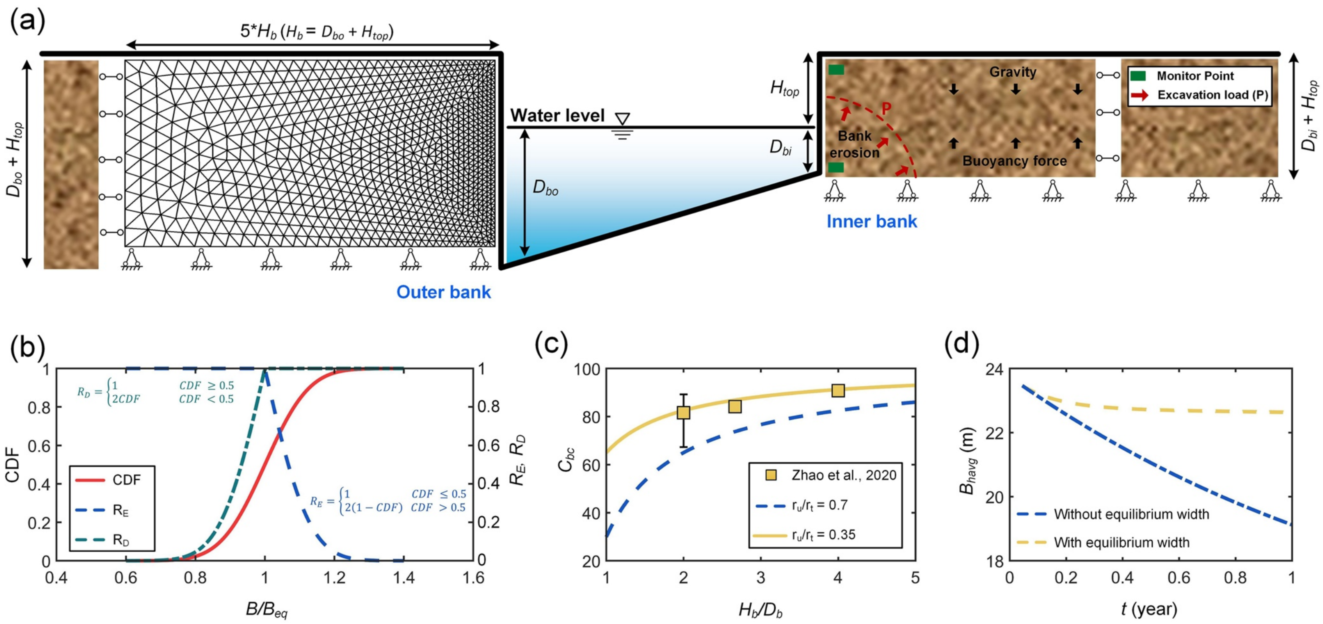

Figure 1. (a) Sketch of a meander cross section, showing water depth of outer and inner banks (D_{bo} and D_{bi}), upper bank height (H_{top}), and the finite element meshes and boundary conditions applied to simulate bank collapse through the stress-strain analysis. The bank base is assumed to consist of a flat nondeformable boundary in both horizontal and vertical directions, while the landward bank edge is fixed in the horizontal direction but allowed to deform vertically. (b) Cumulative density function of half channel width B scaled by the equilibrium width B_{eq} and the corresponding parameters R_E and R_D, computed for a normal distribution with mean B_{eq}, and a standard deviation $0.1B_{\mathrm{eq}}$. (c) Relation between the ratio of bank height H_b ($=D_b + H_{\mathrm{top}}$) to near-bank water depth D_b and the contribution of bank collapse to the overall bank retreat C_b. (d) Time evolution of the reach-averaged half channel width, B_{havg}, computed by either constraining probabilistically erosion and deposition at the two banks (R_E and R_D computed assuming a normally distributed CFD of B/B_{eq}) or simply setting $R_E = R_D = 1$. The initially constant channel half with is $B_{\mathrm{havg}} = 25$ m, while the initial sinusoidal planform has amplitude $2B_{\mathrm{havg}}$, and wavelength $40B_{\mathrm{havg}}$.

(Lagasse, Zevenbergen, et al., 2004; Mason & Mohrig, 2019; Nanson & Hickin, 1983). The associated width fluctuations can be described by a specific probability density function (PDF) (Lopez Dubon & Lanzoni, 2019) embedding the intrinsic features of the investigated river reach and the surrounding floodplain. Following Lopez Dubon and Lanzoni (2019), a probabilistic approach is thus employed to control channel width, and a PDF is introduced to modulate the rate of bank erosion and deposition. Specifically, the parameters R_E and R_D appearing in relations Equations 1 and 2 are calculated according to the cumulative density function of the selected PDF, that is here assumed Gaussian for the sake of simplicity (Figure 1b).

Bank collapse is modeled by means of either a stress-strain analysis or an empirical function developed from laboratory experiments. Stress-strain analysis employs a set of elasticity equations to describe the relation between soil stress and strain within each bank (Duncan et al., 2014). The Mohr-Coulomb criterion and a critical tensile criterion are used to evaluate the stability of the bank on the basis of soil stress (Gong et al., 2018; Zhao et al., 2019). The bank height, H_b ($=D_b + H_{\mathrm{top}}$) is determined by the sum of near-bank water depth, D_b, and an upper bank height, H_{top}, computed with respect to the water surface level (Figure 1a). To minimize lateral boundary effects on soil stress distribution, the bank width is set to $5H_b$ for both banks. The bank region is discretized using unstructured cells, with higher resolution near the bank edge. At each time step, the net sedimentation rate over each bank is calculated as the difference $\varepsilon_E - \varepsilon_D$; the computational meshes of each bank are then evaluated and adjusted according to the updated bank profile, defined at several monitoring points.

Alternatively, bank collapse has been modeled as a continuous process (Zhao et al., 2020), relating as follows the contribution of bank collapse to bank retreat, C_{bc}, to the ratio of bank height to near-bank water depth, H_b/D_b:

$$C_{\mathrm{bc}} = 1 - \frac{r_u}{r_t}\frac{D_b}{H_b} \tag{3}$$

where r_u is the undermining rate (m/s) of the bank base and r_t is the retreat rate (m/s) of the upper bank border. The ratio r_u/r_t is related to the type of bank failure and soil properties (e.g., soil cohesion and water content). For toppling failures and bare banks made of sand and/or silt, Zhao et al. (2020) suggested to set $r_u/r_t = 0.35$. Given that natural riverbanks are commonly covered by vegetation and comprised of clay and silt, we select a relatively larger value (0.7) of r_u/r_t (Figure 1c).

The erosion rate induced by the near-bank flow is thus amplified by C_{bc} to account for the average effect of bank collapse events, and the bank retreat rate (ε_R) is expressed as:

$$\varepsilon_R = \frac{\varepsilon_E}{0.7}\frac{H_b}{D_b} \quad (4)$$

Present simulations have been carried out choosing an initially constant reach-averaged channel half width B_{havg} and letting the river to evolve starting from an initial sinusoidal planform (with Cartesian wavelength $L_b/B_{\mathrm{havg}} = 40$) and an amplitude A ensuring either small ($A = 2B_{\mathrm{havg}}$) or moderate ($A = 6B_{\mathrm{havg}}$) channel axis curvature at the bend apex. We use the same value for morphodynamic and geotechnical parameters in all runs: mean half width to depth ratio $\beta = 27$, dimensionless sediment grain size $d_s = 0.003$, shields parameter for the reference uniform flow $\tau_u = 0.06$, particle Reynolds number $R_p = 127$, soil cohesion $\sigma_c = 10$ kPa, and critical tensile strength $\sigma_t = 3.5$ kPa. Other geotechnical parameters are the same as Gong et al. (2018). Although it is possible to account for the sheltering effect due to collapsed bank soil by introducing an armoring coefficient (Motta et al., 2014; Parker et al., 2011), we have decided to reduce the number of parameters, embedding armoring effects in the probabilistic approach used to control the channel width (Lopez Dubon & Lanzoni, 2019). Moreover, by integrating the Exner equation over the entire meander length, we account for the continuous variations of the channel slope as a consequence of changes in channel width (Monegaglia & Tubino, 2019). Figure 1d shows the tendency of the reach-averaged channel half width to attain an equilibrium value B_{eq}, when adopting the above described probabilistic approach. In the remaining, we denote as Case A runs performed without bank collapse (i.e., considering only the retreat due to fluvial erosion), Case B runs carried out modeling continuously bank collapse through Equation 4, and Case C runs taking into account the sequence of single bank collapse events through the stress-strain analysis. The suffixes S and M will be used to denote the small or moderate value of the curvature of the bend apex as a result of the amplitude of the initial sinusoidal configuration. Finally, a constant discharge (51 m^3/s) has been used in the present simulations. Its value has been chosen such that both outer and inner bank are partly inundated by water flow during the initial stages of the simulation.

3. Results

As bends evolve from an initial sinuous configuration and bend curvature reaches sufficiently high values, bank collapse tends to localize where the bend experiences the maximum bed shear stress (Figure 2a). The distribution of the positions of bank collapse in the plane (D_b/H_b, x/L_b) can be fitted through a Gaussian PDF, characterized by a "wide-and-flat" shape ($\mu = 0.36$, $\sigma = 0.19$, continuous blue curve in Figure 2a) for small bend curvatures (initial bend amplitude $A = 2B_{\mathrm{havg}}$), and a "narrow-and-steep" shape ($\mu = 0.26$, $\sigma = 0.03$, continuous black curve) for large bend curvatures ($A = 12B_{\mathrm{havg}}$). A qualitatively similar trend is evident when changing the ratio D_b/H_b by means of the upper bank height, H_{top} (dashed blue and black lines in Figure 2a): a decreased ratio D_b/H_b leads to more frequent bank collapses. This typically occurs when bend curvature is relatively low (e.g., during the early stages of simulations carried out with $A = 2B_{\mathrm{havg}}$) and the collapse location is scattered along the bend, lagging either upstream or downstream of the position of the maximum bed shear stress. Under these conditions, the departures of the bed shear stress from the value characterizing a straight configuration are quite small and therefore, it is the ratio D_b/H_b that controls bank stability. Bank collapse due to toppling (Zhao et al., 2020) is expected to occur where D_b/H_b has lower values, leading to a larger bank retreat. On the other hand, as bends evolve or the initial configuration has already a large enough curvature at the bend apex (e.g., for $A = 12B_{\mathrm{havg}}$), bank collapse generally tends to occur nearby the section where the bed shear stress is maximum, independently of the ratio D_b/H_b. This occurs because for relatively sharp bends, the bed shear stress at sections characterized by a small ratio D_b/H_b but with curvatures smaller than that of the bend apex, is too weak to trigger bank collapse, which is consequently dominated by flow-induced erosion rather than bank stability.

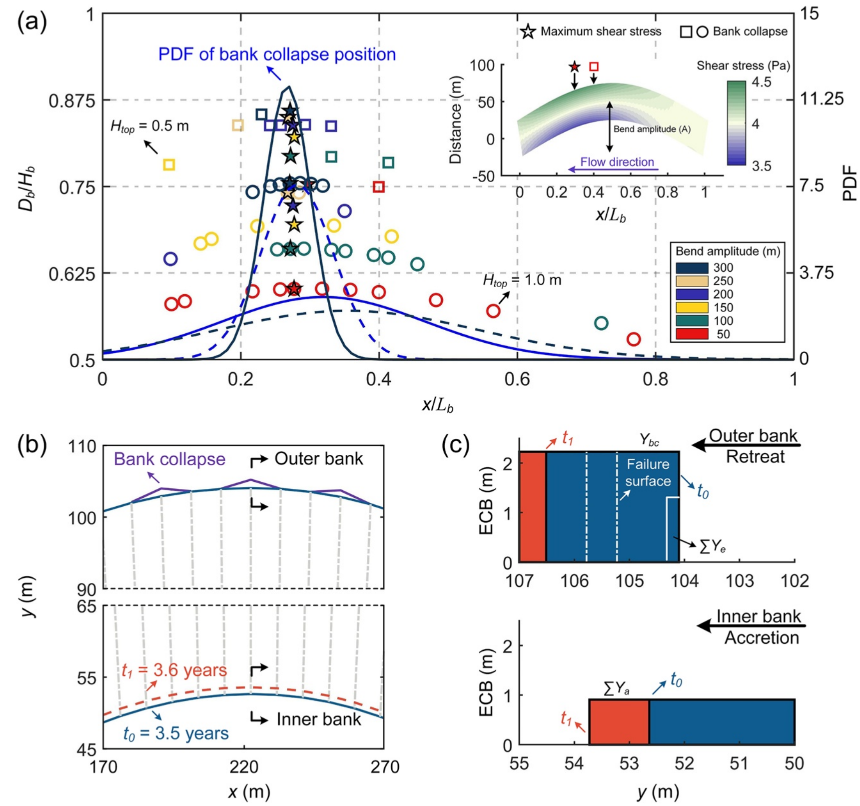

Figure 2. (a) Spatial distribution of simulated bank collapses and (inset) maximum bed shear stress along a meander bend as a function of the ratio between near-bank water depth (D_b) and bank height (H_b). The coordinate x is scaled by the Cartesian meander length, L_b. The inset is a representation of bank collapse location and of maximum shear stress distribution along the bend. Simulations have been carried out with an initial bend amplitude A changing from $2B_{\text{havg}}$ to $12B_{\text{havg}}$ ($B_{\text{havg}} = 25$ m), and upper bank height H_{top} equal to either 0.5 or 1 m. The fitted curves are normal probability density functions of the position of bank collapses: blue ($\mu = 0.36$, $\sigma = 0.19$) and black ($\mu = 0.26$, $\sigma = 0.03$) continuous lines correspond to bend amplitudes of $2B_{\text{havg}}$ and $12B_{\text{havg}}$, respectively; blue ($\mu = 0.28$, $\sigma = 0.1$) and black ($\mu = 0.32$, $\sigma = 0.15$) dashed lines correspond to an upper bank height of 1 and 0.5 m, respectively. Circles correspond to an upper bank height of 1.0 m, and squares correspond to an upper bank height of 0.5 m. Stars represent the maximum shear stress. (b and c) Plan- and cross-sectional view of bend migration, induced by the interplay between bank erosion, collapse, and accretion. The blue continuous line ($t_0 = 3.5$ years) and red dashed line ($t_1 = 3.6$ years) in plot (b) are at the same time as in Figure 3c, when three bank collapse events occur, indicated by the white dashed line in plot (c). The vertical axis ECB represents Elevation with respect to Channel Bottom in front of the bank. Y_{bc} is the retreat driven by an individual bank collapse event, Y_e the retreat driven by bank erosion (occurring at every time step), and Y_a the advance driven by bank accretion (also occurring at every time step).

Although the inclusion of bank collapse eventually leads to pre-cutoff meander planforms similar to those usually computed by velocity-based, continuous erosion models, the effect on migration rates is evident and depends on bend curvature and how the adopted model accounts for bank collapse. For small bend curvatures (e.g., in the early stages of runs B_S and C_S), bank collapse evaluated by stress-strain analysis tends to enhance meander migration, while a slightly lower migration rate is observed when bank collapse is modeled through the parametrization provided by Equation 3. For large bend curvature (e.g., Cases B_M and C_M, and later stages of Cases B_S and C_S), bank collapse increases meander migration, independently of the adopted model. Figure S1 and Text S1 provides a detailed description of the planforms obtained with different bank retreat descriptions. Also, the evolution of channel width toward an asymptotic state depends on the bank retreat model. Although bank collapse eventually leads to an equilibrium width, its effect on the magnitude of erosion/accretion rate is evident. For example, in the presence of small curvatures and modeling continuous bank erosion/collapse, the regime of bank interaction may switch from both banks eroding (early stages of Case B_S) to bank pull (faster outer bank migration) until the asymptotic constant width is reached (Figure 3a). In contrast, a sudden decrease in bank migration is observed immediately after

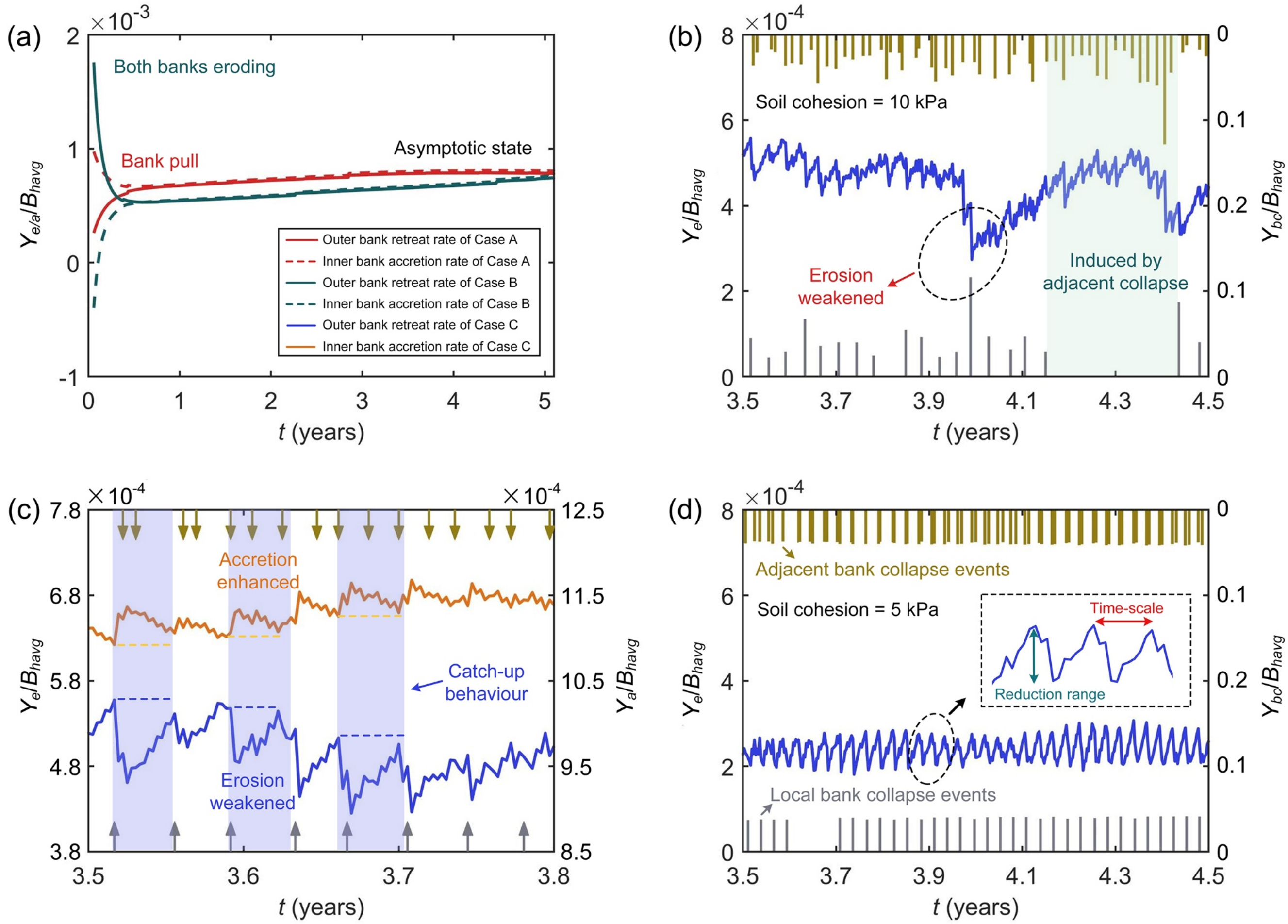

Figure 3. (a) Temporal distribution of the distance of bend apex migration driven by the interplay of flow-induced bank erosion Y_e and bank accretion Y_a at each time step. (b and d) Temporal distribution of the retreat due to flow-induced bank erosion Y_e and the individual bank collapse event Y_{bc} for different values of soil cohesion σ_c, namely (b) 10 kPa and (d) 5 kPa. Y_e, Y_a, and Y_{bc} are measured in the direction normal to the channel axis from previous bank line and shown in Figure 2c. (b) Enlarged view of the catch-up behavior (corresponds to the shaded areas of Figure S1e of supporting information). The bars in plots (b and d) correspond to the timing (indicated by x-axis) and scale (indicated by the dimensionless distance $Y_{\mathrm{bc}}/B_{\mathrm{havg}}$) of the local (bend apex, lower gray bar) and adjacent (upper brown bar) bank collapse events. (c) Temporal distribution of the overall extent of bend apex migration due to erosion Y_e and accretion Y_a. The arrows in plot (c) correspond to bank collapse events occurring at the bend apex (lower gray arrow) and adjacent (one mesh cell) to the bend apex (upper brown arrow). The various quantities on the ordinate axis have been scaled by the reach-averaged half channel width, B_{havg}. The colors of lines are as follows: red, Case A; green, Case B; blue and orange, Case C.

each bank collapse evaluated by stress-strain analysis, and the erosion rate curve fluctuates as a result of bank collapse events occurring either upstream or downstream (Figure 3b). Since bank collapse is massive and intermittent (compared to the continuous flow-induced bank erosion, see Figure 2b), the migration of meander bends can be described as a cycle consisting of a sudden retreat at the outer bank, followed by a catch-up behavior characterized by the co-occurrence of a weakened outer bank erosion and an enhanced inner bank accretion (Figure 3c). The above catch-up behavior is not only related to a given localized bank collapse, but is also affected by upstream/downstream collapse events. Specifically, the higher the soil cohesion, the less frequent and more massive are the bank collapses, leading to a longer time-scale and smaller catch-up extent (Figures 3b and 3d).

For individual bends, model results show that for all three cases the dimensionless local curvature (B_{avg}/R) goes from zero (upstream inflection point) to a large value (apex point) and back to zero (downstream inflection point), and the migration rate, R_m^* ($=R_m$ / B_{avg}) is highly variable (Figure 4). This tendency agrees qualitatively with field observations where for the same bend, local migration rate increased with local

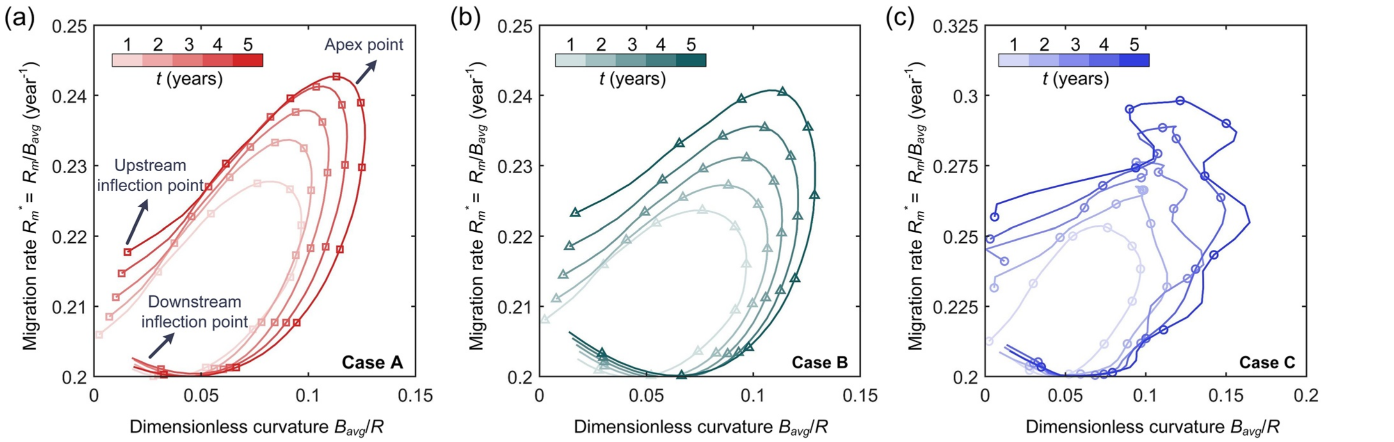

Figure 4. Local migration rate, R_m^*, versus local dimensionless curvature (B_{avg}/R) at different times for data derived from present numerical simulations: (a) Case A, (b) Case B, and (c) Case C. The local migration rate is calculated along a direction perpendicular to the centerline (Sylvester et al., 2019). Faster migration rate within the model can be explained by use of a constant flow discharge in the model. In reality, the channel is only occasionally subject to flood events. An intermittency factor (depending on the hydrological regime of the investigated river) has then to be used (Paola et al., 1992) for ensuring a matching between computed and observed migration rates.

curvature (Sylvester et al., 2019), at least for values of B_{avg}/R up to 0.15. The relatively higher migration rate from the upstream inflection point to the apex point indicates that the planimetric pattern of the simulated meandering river is skewed upstream (see Figure S2a of supporting information). The inclusion of bank collapse through stress-strain analysis affects the curvature-migration relation, as a result of the intermittent nature of collapse events (Case C of Figure 4). When bank collapse occurs, the local curvature and migration rate changes abruptly, accounting for the irregular curve between local curvature and migration rate. As bends evolve, the curvature-migration curve becomes more irregular near the apex point (e.g., at year 5), since bank collapse tends to localize where the bend experiences the maximum bed shear stress (Figure 2a). Model results also suggest that meandering channels follow an evolutionary trend whereby R_m^* first reaches a maximum as the dimensionless local radius of curvature, $R^*(=R\ /\ B_{avg})$ grows, and then decreases with a concomitant increase of R^*, thus yielding a hysteresis loop (see Figure S2 and Text S2 in supporting information).

4. Discussion

The present model suggests that bank collapse, and consequently, maximum bank retreat rates do not necessarily occur where bed shear stress is maximum (Figure 2a), thus challenging the widely adopted linear relation between bank retreat and excess shear stress or flow velocity (e.g., Ikeda et al., 1981). In addition, since bank stability is related to the ratio D_b/H_b (Simon et al., 2000; Zhao et al., 2020), which constantly changes along the bend and with bend evolution (due to variation in water depth), representations of bank collapse as a function of bank slope and/or upper bank height are debatable when simulating in detail meander morphodynamics. Bank collapse speeds up the migration rate of meanders, enhancing bend amplification and therefore leading to an increase in channel axis curvature. The latter, in turn, regulates bank collapse location. As a bend evolves from an initial sinuous configuration with small curvature, the initially scattered bank collapse events progressively tend to concentrate nearby the section where the bed shear stress is maximum. Our results also provide evidence that for a small-curvature bend, a simplified representation of bank collapse as a continuous process (Equation 3) is inaccurate in the short-term, since meander migration is essentially a discontinuous catch-up behavior (Mason & Mohrig, 2019; Nanson & Hickin, 1983). Therefore, although long-term modeling of meanders can efficiently simulate bank retreat as a continuous process, the short-term evolution cannot neglect bank collapse.

Our study thus highlights the need to describe bank collapse events when simulating meander migration, in order to obtain a quantitatively correct estimate of the rates of bank retreat. The model incorporates the interaction between bank collapse and bend planform with a computationally sustainable effort, at least for short- to medium-term predictions. On the basis of the simulations, we suggest that a typical cycle of catch-up behavior describes meander migration driven by bank collapse. During Stage I, a single or a series of bank collapses causes the formation of an initial embayment, whose location and size depend on the bend curvature and the ratio D_b/H_b. At this stage, cross sections affected by bank collapse events experience an increase in channel width. During Stage II, the increased channel width modulates bank erosion/collapse, promotes deposition, and therefore leads to a catch-up behavior between inner and outer banks. The channel width keeps reducing until the deposition rate at the inner bank is small enough. Since the accretion rate of the inner bank is considerably smaller than the retreat rate of the outer bank, a time lag is expected before channel width reaches its equilibrium value. This leads to an increase in erosion rates of adjacent cross sections, and therefore smooths the collapse-induced embayment and speeds up the migration rate of the whole bend. During Stage III, one evolution cycle is completed, and the meander migrates either upstream or downstream, depending on the phase lag between the bend apex and the peak flow location (Lanzoni & Seminara, 2006). As meanders progressively elongate, an asymptotic state may be approached where bank erosion and deposition occur at nearly equal rates, in accordance with the numerical results obtained by Eke, Parker, and Shimizu (2014). Catch-up behavior has been described by Nanson and Hickin (1983) and Mason and Mohrig (2019) on the basis of field observations. We suggest that meander migration should be interpreted as the interplay between bank pull (bank collapse at the outer bank) and bar push (bank accretion at the inner bank) in discrete steps (i.e., catch-up concept). Because of intermittent bank collapses (Figure 3), the instantaneous outer bank erosion rate is never equal to the inner bank deposition rate over the short-term scale (i.e., several floods), and a catch-up behavior rather than an asymptotic state is a more realistic representation of natural rivers. The channel banks are in general morphologically inactive for long periods of time. They are subject to relevant changes as a result of floods. In particular, bank collapse commonly occurs during the recession period of flood events causing large retreat at the outer bank (Simon et al., 2000), followed by inner bank accretion during periods of below-average flows. When using a constant formative discharge (as assumed in the present study), the effect of a varying hydrological forcing can be accounted for by introducing an intermittency factor corresponding to the fraction of time the channel is actually experiencing flood conditions (Paola et al., 1992; Parker et al., 1998). In the general scenario considered here, this intermittency factor is set equal to 1. Therefore, the time-scale typical of the catch-up behavior within the model (months) is certainly faster than reported in field observations (years, e.g., Mason & Mohring, 2019).

The proposed model is able to capture the peak in migration rate for $2 < R^* < 4$, a common feature of meandering rivers, but does not describe accurately the subsequent reduction in R_m^* as the radius of curvature decreases to small values (Figure S2 in supporting information). A similar result has also been reported by Eke, Czapiga, et al. (2014), who found a weakened tendency of R_m^* to decrease after reaching a peak value, thus yielding a hysteresis loop rather than a bell shaped curve. This may be due to the limitations of the mathematical model describing the flow field in the bend. For high bend curvatures, the present linearized flow field model is in fact not valid anymore, and the along bend distribution of the secondary currents may vary significantly with respect to mild bends and does no longer vary in the lower range of R^* values, owning to the saturation effect described by Blanckaert (2011) and Ottevanger et al. (2013). Further research is thus needed to unravel the interactions between bank erosion/collapse and bend migration, and to fully elucidate the relation $R_m^* \sim R^*$. Finally, the effect of collapsed bank soil is not explicitly accounted for in this model. Clearly, the sediment deposits (slump blocks) consequent to bank collapse may prevent or promote bank erosion (Hackney et al., 2015; Wood et al., 2001). Since deposits of collapsed sediment may play a key role in determining bank erosion rates, research is needed to incorporate their effect in numerical models.

5. Summary

The interactions between bank erosion and meander migration are essential. Bend curvature and the associated near-bank hydraulics determine the location of bank collapse, which in turn adds to flow-induced erosion, speeding up migration rates and driving changes in bend curvature. As a bend evolves from a small amplitude sinusoidal configuration, the initially scattered bank collapse events concentrate at the outer bank and converge toward the section where the bed shear stress attains a maximum, implying a transition from a bank-stability-dominated state (controlled by the ratio between near-bank water depth and bank height) to a hydraulic-dominated state (dictated by the near-bank distribution of bed shear stress). The present model illustrates the catch-up behavior observed in nature, driven by intermittent outer bank collapse and continuous inner bank accretion. For the same bend, local migration rate increased with local curvature and the inclusion of bank collapse affects the curvature-migration relation, as a result of the intermittent nature of collapse events. Overall, this research improves our understanding of the interaction between bank collapse and meander migration, and therefore provides new insights on alluvial river evolution.

Data Availability Statement

All data shown in the figures of this research can be found in Zhao et al. (2020). The code developed in this study is available on GitHub website (https://doi.org/10.5281/zenodo.4898932).

Acknowledgments
This research is supported by National Natural Science Foundation of China (51925905, 51879095, and 51620105005). The authors appreciate *NeSI* (New Zealand eScience Infrastructure) for supporting our numerical simulations. Special thanks are given to *Alvise Finotello*, who provides suggestions for figures and data analysis. Constructive and insightful comments by Zoltán Sylvester significantly improved the manuscript.

References

Asahi, K., Shimizu, Y., Nelson, J., & Parker, G. (2013). Numerical simulation of river meandering with self-evolving banks. *Journal of Geophysical Research: Earth Surface*, *118*(4), 2208–2229. https://doi.org/10.1002/jgrf.20150

Blanckaert, K. (2011). Hydrodynamic processes in sharp meander bends and their morphological implications. *Journal of Geophysical Research*, *116*(F1). https://doi.org/10.1029/2010jf001806

Blondeaux, P., & Seminara, G. (1985). A unified bar–bend theory of river meanders. *Journal of Fluid Mechanics*, *157*, 449–470. https://doi.org/10.1017/s0022112085002440

Darby, S. E., Alabyan, A. M., & Wiel, Van de, M. J. (2002). Numerical simulation of bank erosion and channel migration in meandering rivers. *Water Resources Research*, *38*(9), 1163. https://doi.org/10.1029/2001wr000602

Darby, S. E., & Thorne, C. R. (1994). Prediction of tension crack location and riverbank erosion hazards along destabilized channels. *Earth Surface Processes and Landforms*, *19*(3), 233–245. https://doi.org/10.1002/esp.3290190304

Duncan, J. M., Wright, S. G., & Brandon, T. L. (2014). *Soil strength and slope stability*. John Wiley & Sons.

Eke, E. C., Czapiga, M. J., Viparelli, E., Shimizu, Y., Imran, J., Sun, T., & Parker, G. (2014). Coevolution of width and sinuosity in meandering rivers. *Journal of Fluid Mechanics*, *760*, 127–174. https://doi.org/10.1017/jfm.2014.556

Eke, E. C., Parker, G., & Shimizu, Y. (2014). Numerical modeling of erosional and depositional bank processes in migrating river bends with self-formed width: Morphodynamics of bar push and bank pull. *Journal of Geophysical Research: Earth Surface*, *119*(7), 1455–1483. https://doi.org/10.1002/2013jf003020

Finotello, A., Lanzoni, S., Ghinassi, M., Marani, M., Rinaldo, A., & D'Alpaos, A. (2018). Field migration rates of tidal meanders recapitulate fluvial morphodynamics. *Proceedings of the National Academy of Sciences of the United States of America*, *115*(7), 1463–1468. https://doi.org/10.1073/pnas.1711330115

Frascati, A., & Lanzoni, S. (2009). Morphodynamic regime and long-term evolution of meandering rivers. *Journal of Geophysical Research*, *114*, F020021. https://doi.org/10.1029/2008jf001101

Frascati, A., & Lanzoni, S. (2013). A mathematical model for meandering rivers with varying width. *Journal of Geophysical Research: Earth Surface*, *118*(3), 1641–1657. https://doi.org/10.1002/jgrf.20084

Furbish, D. J. (1988). River-bend curvature and migration: How are they related? *Geology*, *16*(8), 752–755. https://doi.org/10.1130/0091-7613(1988)016<0752:rbcamh>2.3.co;2

Gong, Z., Zhao, K., Zhang, C., Dai, W., Coco, G., & Zhou, Z. (2018). The role of bank collapse on tidal creek ontogeny: A novel process-based model for bank retreat. *Geomorphology*, *311*, 13–26. https://doi.org/10.1016/j.geomorph.2018.03.016

Hackney, C., Best, J., Leyland, J., Darby, S. E., Parsons, D., Aalto, R., & Nicholas, A. (2015). Modulation of outer bank erosion by slump blocks: Disentangling the protective and destructive role of failed material on the three-dimensional flow structure. *Geophysical Research Letters*, *42*(24), 10–663. https://doi.org/10.1002/2015gl066481

Hackney, C. R., Darby, S. E., Parsons, D. R., Leyland, J., Best, J. L., Aalto, R., et al. (2020). River bank instability from unsustainable sand mining in the lower Mekong River. *Nature Sustainability*, *3*(3), 217–225. https://doi.org/10.1038/s41893-019-0455-3

Hooke, J. M. (1979). An analysis of the processes of river bank erosion. *Journal of Hydrology*, *42*(1), 39–62. https://doi.org/10.1016/0022-1694(79)90005-2

Howard, A. D. (1996). Modeling channel evolution and floodplain morphology. In M. G. Anderson, D. E. Walling, & P. D. Bates (Eds.), Floodplain processes (pp. 15–62). John Wiley.

Hudson, P. F., & Kesel, R. H. (2000). Channel migration and meander-bend curvature in the lower Mississippi River prior to major human modification. *Geology*, *28*(6), 531–534. https://doi.org/10.1130/0091-7613(2000)028<0531:cmambc>2.3.co;2

Ikeda, S., Parker, G., & Sawai, K. (1981). Bend theory of river meanders. Part 1. Linear development. *Journal of Fluid Mechanics*, *112*, 363–377. https://doi.org/10.1017/s0022112081000451

Lagasse, P. F., Spitz, W. J., Zevenbergen, L. W., Zachmann, D. (2004). *Handbook for predicting stream meander migration*. Transportation Research Board, Owen Ayres & Associates.

Lagasse, P. F., Zevenbergen, L. W., Spitz, W. J., & Thorne, C. R. (2004). *Methodology for predicting channel migration (No. NCHRP Project 24-16)*.

Langendoen, E. J., Mendoza, A., Abad, J. D., Tassi, P., Wang, D., Ata, R., et al. (2016). Improved numerical modeling of morphodynamics of rivers with steep banks. *Advances in Water Resources*, *93*, 4–14. https://doi.org/10.1016/j.advwatres.2015.04.002

Lanzoni, S., & Seminara, G. (2006). On the nature of meander instability. *Journal of Geophysical Research*, *111*, F04006. https://doi.org/10.1029/2005jf000416

Lopez Dubon, S., & Lanzoni, S. (2019). Meandering evolution and width variations: A physics-statistics-based modeling approach. *Water Resources Research*, *55*, 76–94. https://doi.org/10.1029/2018WR023639

Mason, J., & Mohrig, D. (2019). Differential bank migration and the maintenance of channel width in meandering river bends. *Geology*, *47*(12), 1136–1140. https://doi.org/10.1130/g46651.1

Monegaglia, F., & Tubino, M. (2019). The hydraulic geometry of evolving meandering rivers. *Journal of Geophysical Research: Earth Surface*, *124*, 1–26. https://doi.org/10.1029/2019JF00530910.1029/2019jf005309

Motta, D., Langendoen, E. J., Abad, J. D., & García, M. H. (2014). Modification of meander migration by bank failures. *Journal of Geophysical Research: Earth Surface*, *119*(5), 1026–1042. https://doi.org/10.1002/2013jf002952

Nanson, G. C., & Hickin, E. J. (1983). Channel migration and incision on the Beatton River. *Journal of Hydraulic Engineering*, *109*(3), 327–337. https://doi.org/10.1061/(asce)0733-9429(1983)109:3(327)

Odgaard, A. J. (1987). Streambank erosion along two rivers in Iowa. *Water Resources Research*, *23*(7), 1225–1236. https://doi.org/10.1029/wr023i007p01225

Ottevanger, W., Blanckaert, K., Uijttewaal, W. S. J., & Vriend, de, H. J. (2013). Meander dynamics: A reduced-order nonlinear model without curvature restrictions for flow and bed morphology. *Journal of Geophysical Research: Earth Surface*, *118*(2), 1118–1131. https://doi.org/10.1002/jgrf.20080

Paola, C., Heller, P. L., & Angevine, C. L. (1992). The large-scale dynamics of grain-size variation in alluvial basins, 1: Theory. *Basin Research*, *4*(2), 73–90. https://doi.org/10.1111/j.1365-2117.1992.tb00145.x

Parker, G., Paola, C., Whipple, K. X., & Mohrig, D. (1998). Alluvial fans formed by channelized fluvial and sheet flow. I: Theory. *Journal of Hydraulic Engineering*, *124*(10), 985–995. https://doi.org/10.1061/(asce)0733-9429(1998)124:10(985)

Parker, G., Shimizu, Y., Wilkerson, G. V., Eke, E. C., Abad, J. D., Lauer, J. W., et al. (2011). A new framework for modeling the migration of meandering rivers. *Earth Surface Processes and Landforms*, *36*(1), 70–86. https://doi.org/10.1002/esp.2113

Patsinghasanee, S., Kimura, I., Shimizu, Y., & Nabi, M. (2018). Experiments and modelling of cantilever failures for cohesive riverbanks. *Journal of Hydraulic Research*, *56*(1), 76–95. https://doi.org/10.1080/00221686.2017.1300194

Piégay, H., Darby, S. E., Mosselman, E., & Surian, N. (2005). A review of techniques available for delimiting the erodible river corridor: A sustainable approach to managing bank erosion. *River Research and Applications*, *21*(7), 773–789. https://doi.org/10.1002/rra.881

Samadi, A., Amiri-Tokaldany, E., Davoudi, M. H., & Darby, S. E. (2013). Experimental and numerical investigation of the stability of overhanging riverbanks. *Geomorphology*, *184*(0), 1–19. https://doi.org/10.1016/j.geomorph.2012.03.033

Seminara, G. (2006). Meanders. *Journal of Fluid Mechanics*, *554*, 271–297. https://doi.org/10.1017/s0022112006008925

Simon, A., Curini, A., Darby, S. E., & Langendoen, E. J. (2000). Bank and near-bank processes in an incised channel. *Geomorphology*, *35*(3–4), 193–217. https://doi.org/10.1016/s0169-555x(00)00036-2

Sylvester, Z., Durkin, P., & Covault, J. A. (2019). High curvatures drive river meandering. *Geology*, *47*(3), 263–266. https://doi.org/10.1130/g45608.1

Wood, A. L., Simon, A., Downs, P. W., & Thorne, C. R. (2001). Bank-toe processes in incised channels: The role of apparent cohesion in the entrainment of failed bank materials. *Hydrological Processes*, *15*(1), 39–61. https://doi.org/10.1002/hyp.151

Zhao, K., Gong, Z., Xu, F., Zhou, Z., Zhang, C. K., Perillo, G., & Coco, G. (2019). The role of collapsed bank soil on tidal channel evolution: A process-based model involving bank collapse and sediment dynamics. *Water Resources Research*, *55*(11), 9051–9071. https://doi.org/10.1029/2019wr025514

Zhao, K., Gong, Z., Zhang, K., Wang, K., Jin, C., Zhou, Z., et al. (2020). Laboratory experiments of bank collapse: The role of bank height and near-bank water depth. *Journal of Geophysical Research: Earth Surface*, *125*(5). https://doi.org/10.1029/2019jf005281

Zolezzi, G., Luchi, R., & Tubino, M. (2012). Modeling morphodynamic processes in meandering rivers with spatial width variations. *Reviews of Geophysics*, *50*(RG4005), 1–24. https://doi.org/10.1029/2012rg000392

Zolezzi, G., & Seminara, G. (2001). Downstream and upstream influence in river meandering. Part 1. General theory and application to overdeepening. *Journal of Fluid Mechanics*, *438*(13), 183–211. https://doi.org/10.1017/s002211200100427x